Int. J. Heat Mass Transfer. Vol. 15, pp. 2011–2025. Pergamon Press 1972. Printed in Great Britain

BOILING FROM SMALL CYLINDERS*

NANIK BAKHRU
IBM Corporation, Hopewell Junction, New York 12533, U.S.A.
and
JOHN H. LIENHARD
Dept. of Mechanical Engineering, University of Kentucky, Lexington, Kentucky 40506, U.S.A.

(*Received* 27 *September* 1971)

Abstract—Heat transfer is observed as a function of temperature on small horizontal wires in water and four organic liquids. When the wire radius is sufficiently small, the hydrodynamic transitions in the boiling curve disappear and the curve becomes monotonic. Three modes of heat removal are identified for the monotonic curve and described analytically: a natural convection mode, a mixed film boiling and natural convection mode, and a pure film boiling mode. Nucleate boiling does not occur on the small wires.

The study was motivated by an interest in predicting the behavior of large heaters at low gravity. The application of the present results to such circumstances is therefore discussed. It is proposed that the peak and minimum heat fluxes will vanish at low gravity as well as on small wires.

NOMENCLATURE

Bi, Biot number, $hR/2k_w$;
$f(R')$, a function of R';
g, acceleration of a system in a force field;
h, heat transfer coefficient, q/θ_e;
h_{fg}, latent heat of vaporization;
h^*_{fg}, latent heat of evaporation plus 34 per cent of the sensible heat of vapor at heater wall;
k, k_g, k_w, thermal conductivity of liquid, vapor and heater, respectively;
Nu, Nusselt number, $2hR/k$
Pe, dimensionless velocity, or Péclét number, defined by equation (8);
p, pressure;
q, average heat flux on the entire heater. Also heat flux on the unblanketed portion of the heater when used with q_b;
q_b, heat flux on the blanketed portion of the wire;
q_{max}, q_{min}, peak and minimum boiling heat fluxes, respectively;
r, radius of a bubble;
q_{max_F}, Zuber's predicted peak heat flux for a flat plate;
R, characteristic dimension, usually used to denote the radius of a cylindrical wire;
R', dimensionless characteristic dimension (usually the radius), $R[g(\rho_f - \rho_g)/\sigma]^{\frac{1}{2}}$;
Ra^*, modified Rayleigh number, equation (16);
T, temperature;
T_w, heater surface temperature;
ΔT, wall superheat, $T_w - T_{sat}$;
ΔT_{ov}, temperature overshoot, T at nucleation minus minimum T for q beyond nucleation;
t, time;
u, speed of vapor patch propagation;
v_{fg}, $(1/\rho_g) - (1/\rho_f)$;

* This work was supported by NASA Grant NGR/18-001-035, under the cognizance of the NASA Lewis Research Center. The paper is extracted from the first author's doctoral dissertation at the University of Kentucky.

x, x_b, axial distance coordinate; subscript b denotes reversed coordinate under the blanketed portion of the wire;
y, distance measured from solid wall into liquid.

Greek symbols

α, thermal diffusivity of heater;
Λ, a dimensionless function, $2\sigma h v_{fg} T_{sat}/\Delta T h_{fg} k$;
μ, viscosity of vapor;
ρ_f, ρ_g, saturated liquid and vapor densities, respectively;
σ, surface tension between a saturated liquid and its vapor;
θ, temperature measured above T_{sat};
θ_e, equilibrium temperature in the wire, q/h;
θ_0, vapor patch triggering temperature;
Θ, Θ_0, dimensionless temperatures, θ/θ_e and θ_0/θ_e, respectively;
ξ, ξ_b, dimensionless axial parameters defined after equation (10).

General subscripts

b, denoting conditions related to the portion of heater blanketed by vapor;
sat, denoting conditions at saturation.

INTRODUCTION

THE EARLY experiments of Nukiyama [1] and of Drew and Mueller [2] demonstrated that the plot of heat flux, q, against the liquid superheat at the heater surface, ΔT, exhibited local maximum and minimum points. This discovery set the stage for a program of study that has lasted a third of a century. Since heat transfer is remarkably efficient near the local maximum, great effort has been directed toward predicting this limiting heat flux.

In 1948 Kutateladze [3] discussed the mechanism that dictated these extrema, and in 1958 Zuber (see e.g. [4]) provided an analytical description of q_{max} and q_{min} for an infinite flat plate heater. For q_{max} he found

$$q_{max_F} \simeq \frac{\pi}{24} \rho_g^{\frac{1}{2}} h_{fg} \sqrt[4]{(\sigma g(\rho_f - \rho_g))}. \quad (1)$$

The Zuber–Kutateladze theory says that q_{max} occurs when the vapor jets leaving the surface becomes Helmholtz unstable. It also says that the jets are arranged on a grid that is sized according to the Taylor unstable wavelength in the liquid–vapor interface. These instabilities arise as a consequence of inertial, interfacial, and buoyant forces.

The hydrodynamic theory has also been formulated for q_{max} in two finite geometries (cylinders [5] and spheres [6]) and for q_{min} on cylinders [7, 8]. For finite geometries it was shown independently by Bobrovich *et al.* [9] and by Lienhard and Watanabe [10] that if the characteristic dimension of a body is R, then

$$q_{max}/q_{max_F} = f(R') \quad \text{where}$$
$$R' = R\sqrt{[g(\rho_f - \rho_g)/\sigma]}. \quad (2)$$

Equation (2) has been shown [11] to apply as long as: the contact angle is small, the system is not close to the critical pressure, and the viscosity of the liquid is not great.

Under conditions of very low gravity, or for very small heaters, R' (which characterizes the ratio of buoyant forces to surface tension forces) becomes small. Figure 1 shows the q_{max} correlation, equation (2), as applied to about 900 horizontal cylinder data in [5]. In this case, an R' based on the radius, R, must exceed 0·15 if the Zuber–Kutateladze wave mechanisms which define q_{max} are to stay intact. For smaller values of R', surface tension so over balances inertia that these mechanisms deteriorate, and a sampling of data by Kutateladze *et al.* [12], Sun and Lienhard [5], and Siegel and Howell [13] no longer correlate on q_{max}/q_{max_F} vs. R' coordinates.

It was likewise shown in [8] that there is still good visual evidence of the wave stability mechanisms for all $R' \geqslant 0{\cdot}12$, during film

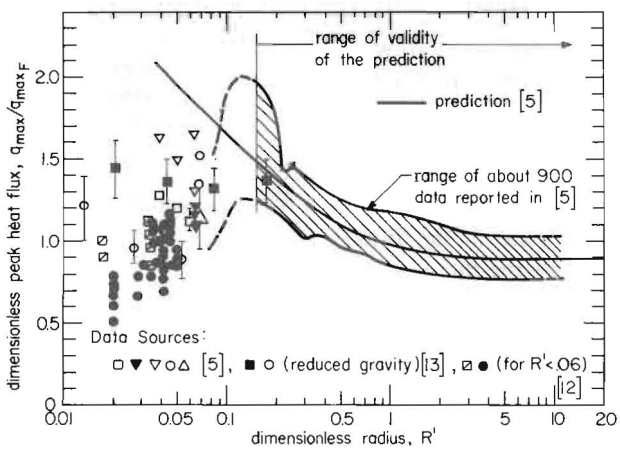

FIG. 1. Deterioration of q_{max} correlation at small R'.

boiling on horizontal cylinders. But for $R' \leqslant 0{\cdot}06$ these mechanisms cease to be identifiable.

If equation (2) fails, and the Zuber–Kutateladze mechanism fails with it, what exactly happens to the boiling process at small R'? The photographs of Sun [5], of Pitts and Leppert [14], and of Kutateladze *et al.* [12] for small wires provide some clue. Bubbles grow on the wire until they are large enough to buoy off and there is no evidence of the inertial waves that are apparent on large wires. The photographs of Siegel and Usiskin [15] and Siegel and Howell [13] show the same kind of process for greatly reduced gravity. The forces of surface tension and buoyancy remain important, however the process is slowed down and the effects of inertia are greatly reduced. Indeed, the soundtrack of a movie by Siegel and Keshock (associated with [16]) specifically notes the reduced inertia effects in boiling under low gravity.

The problem that we face is then this: "If, at low gravity or for small wires, inertia becomes insignificant and the Zuber–Kutateladze mechanisms fail, what replaces them?" We must now ask what the various investigators who

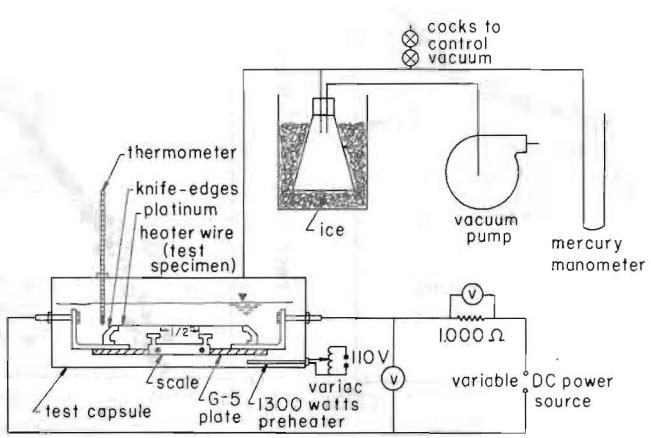

FIG. 2. Schematic representation of experimental apparatus.

have given q_{max} and q_{min} data for low R' have actually observed. Without the inertial wave mechanisms it is hard to see how there could have been any q_{max} or q_{min} points to report.

EXPERIMENT

To answer the question raised in the Introduction we set out to measure the full q vs. ΔT curve for very small wires heating a variety of liquids. The apparatus used to do this is shown in Fig. 2.

A small platinum wire, which serves as both a resistance heater and a resistance thermometer, is suspended in the liquid of interest and boiling is observed at successive heat fluxes. The temperature of the wire was calculated from the resistance which in turn was computed from the ratio of voltage to current, using the method detailed by van Stralen and Sluyter [17]. Since complete details of the experimental method are given by Bakhru [18], we shall only list a few major features of the tests here:

The wires were cleaned in soap and then rinsed in the test liquid. Reagent grade liquids were used in all cases. During actual observations the preheater, which was used to maintain saturation conditions, was momentarily switched off. Since the wires would melt during atmospheric pressure runs in water, the water runs were all made at pressures in the neighborhood of 3 in. Hg abs. The maximum probable error in q was found to be $2\frac{1}{2}$ per cent. The maximum probable error in ΔT varied from

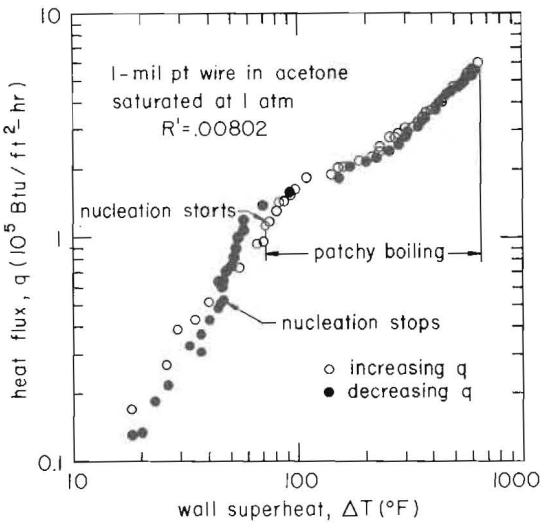

FIG. 4. Boiling curve for 1-mil platinum wire in acetone.

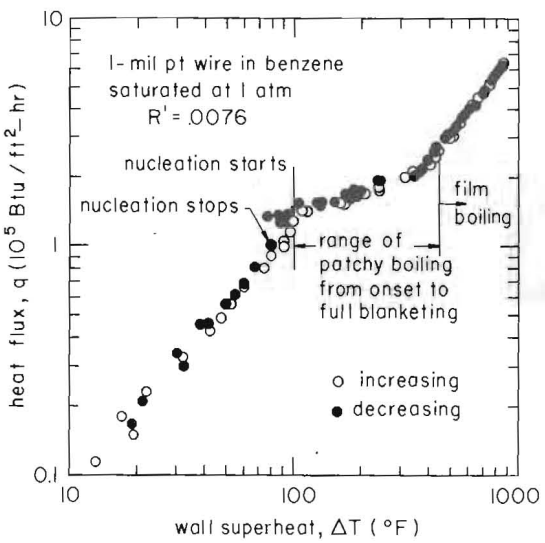

FIG. 3. Boiling curve for 1-mil platinum wire in benzene.

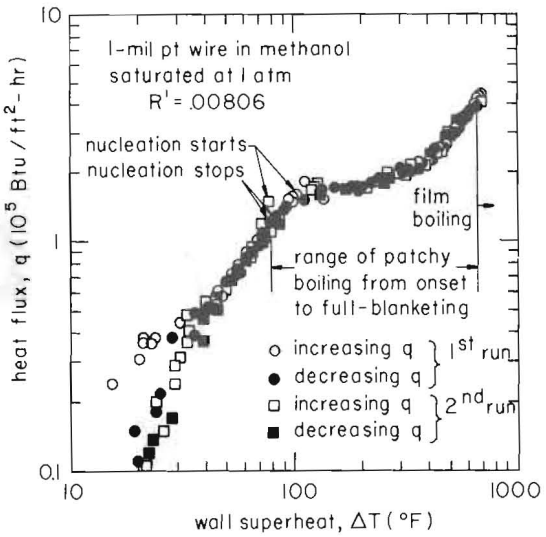

FIG. 5. Boiling curve for 1-mil platinum wire in methanol.

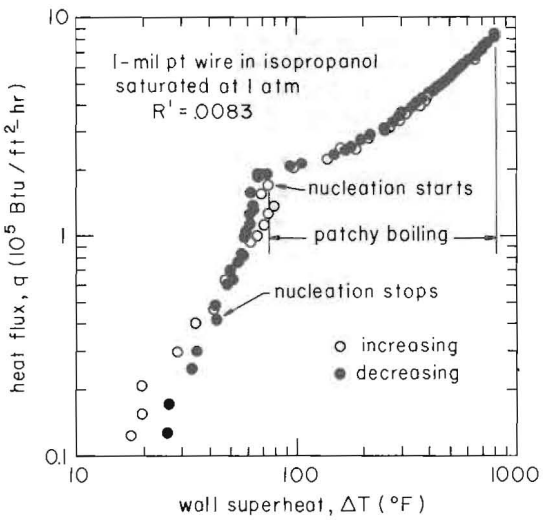

FIG. 6. Boiling curve for 1-mil platinum wire in isopropanol.

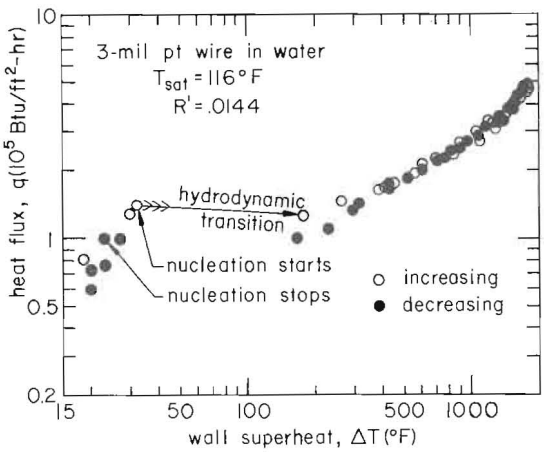

FIG. 8. Boiling curve for 3-mil platinum wire in water.

36 per cent or about $5\frac{1}{2}$ °F at the very lowest ΔT's to 1·8 per cent or about 13 °F at the highest ΔT's.

Our complete raw data are given in the form of 13 boiling curves in Figs. 3–14. These have been arranged in order of increasing R' from 0·0076 up to 0·0806. In each case data are presented for both increasing and decreasing heat flux to expose any hysteresis effects. Figure 5 combines data for two wires under identical conditions to assure reproducibility of results.

The major significance of the present study is readily apparent from these curves. As ΔT is increased on the smaller wires, q rises monotonically without passing through a maximum and minimum. Only as R' increases to about

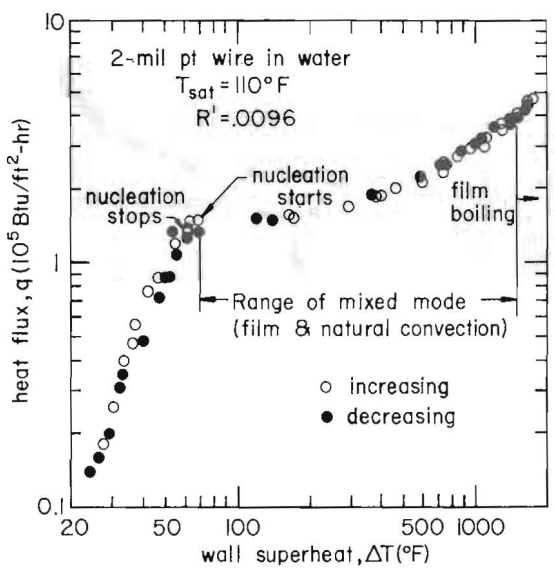

FIG. 7. Boiling curve for 2-mil platinum wire in water.

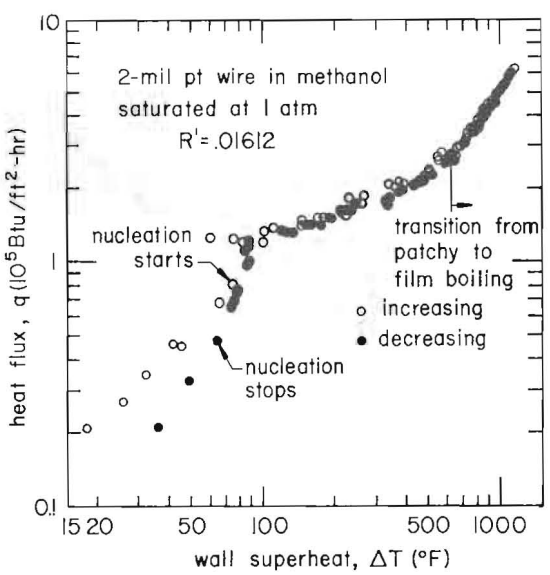

FIG. 9. Boiling curve for 2-mil platinum wire in methanol.

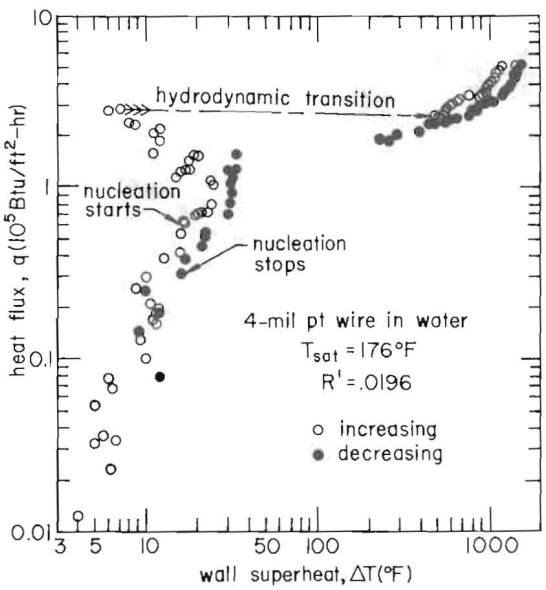

FIG. 10. Boiling curve for 4-mil platinum wire in water.

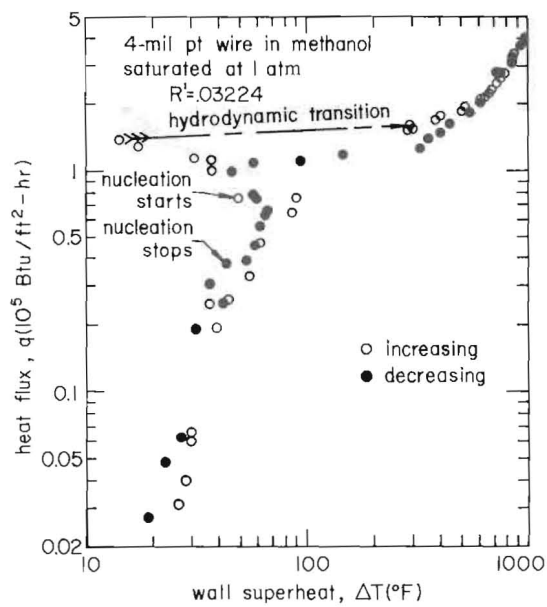

FIG. 12. Boiling curve for 4-mil platinum wire in methanol.

$\frac{1}{10}$ does the conventional boiling curve begin to re-establish itself.

Still and high-speed motion pictures were made during the boiling process. For small R', the still pictures were similar to pictures presented by several previous authors for small wires at high heat fluxes (e.g. [12] and [14]) as well as to those presented for large wires at low gravity (e.g. [13] and [15]). The first nucleation resulted in a bubble which grew and spread horizontally until the wire was partially blanketed with a vapor patch. As q was increased,

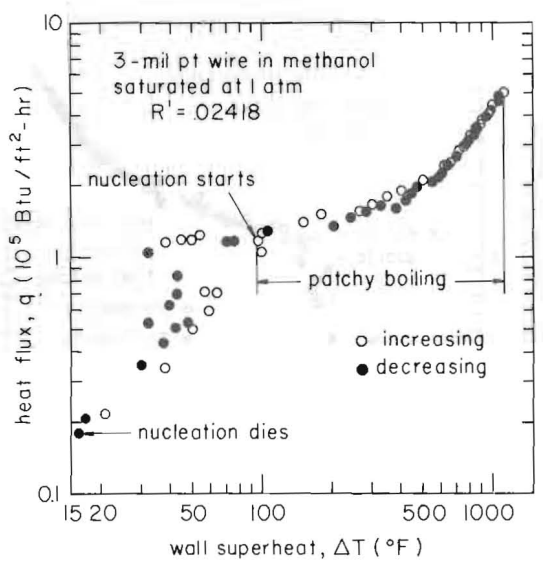

FIG. 11. Boiling curve for 3-mil platinum wire in methanol.

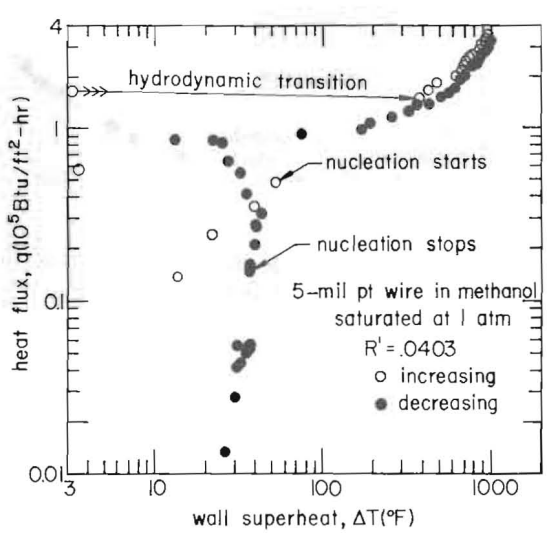

FIG. 13. Boiling curve for 5-mil platinum wire in methanol.

the fraction of the wire covered by vapor increased until the wire was totally blanketed.

The photographs very strongly suggested that the blanketed portions of the wire were fully covered with vapor and that there was no liquid-to-heater contact within them. While these patches are properly to be called "film boiling" they exhibited none of the Taylor wave processes. Instead, vapor removal was accomplished when buoyancy alone overbalanced surface tension, so that fairly large bubbles rose in an irregular way.

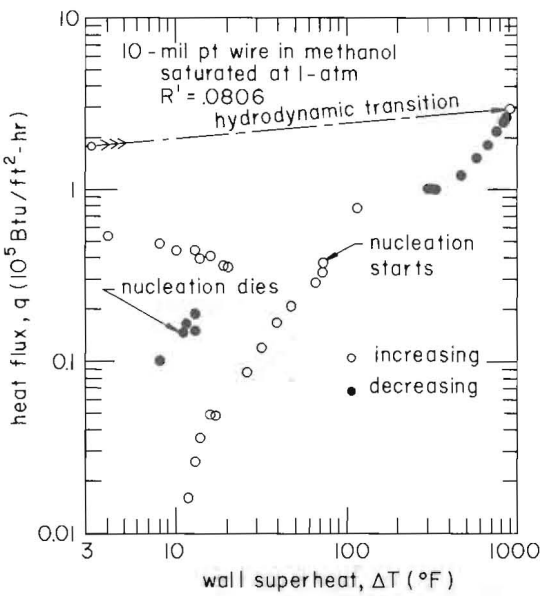

FIG. 14. Boiling curve for 10-mil platinum wire in methanol.

The motion pictures provided details of patch growth and collapse. Figure 15 shows a tracing made from a 10-frame motion picture sequence during the growth of a patch on a 1-mil wire in methanol. In the organic liquids that we used, patches would rapidly grow in this way and then collapse. Thus the vapor patches would flicker on and off from place to place on the wire. However, the patches were very stable in water. They would establish themselves and then

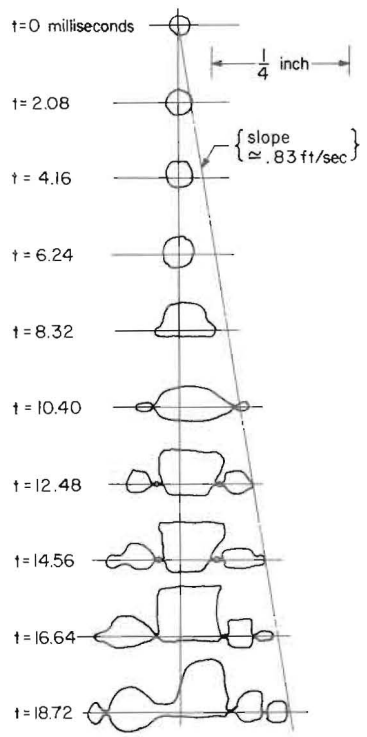

FIG. 15. Vapor patch propagation traced from a ten-frame motion picture sequence. Methanol on a 1-mil platinum wire, $R' = 0{\cdot}008$, $q = 165\,000$ Btu/ft^{2}h.

spread steadily as the heat flux was increased, until the wire was totally blanketed.

The boiling curves show that for $R' \leqslant 0{\cdot}01$ the monotonic small-wire mechanisms are completely established. As R' is increased from 0·01 to about 0·03, two phenomena appear: One is the onset of hydrodynamic transition in the sense that nucleate boiling occurs first, and then undergoes a discontinuous transition to film boiling. The other phenomenon is a temperature overshoot on the rising heat flux curve. The resulting hysteresis in the curve becomes quite pronounced as R' is further increased to 0·08. The hydrodynamic mechanisms, of course, will only be *fully* re-established for R' values of about 0·12 or 0·15—well beyond the range of the present tests.

We thus have four distinct processes to consider in greater detail. They are:

(1) Natural convection from small wires.
(2) The inception of boiling.
(3) The mixed-mode, or combined film-boiling and natural convection, regime.
(4) Film boiling from small wires.

The nucleate and transition boiling regimes do not appear in the list since they do not occur when R' is small.

Of these processes we shall concentrate on the last three. Bakhru's [18] consideration of the natural convection data presented in Figs. 3–14 revealed that they were generally consistent with the results of many investigators, as have been correlated by McAdams [19], and that their scatter was generally comparable. A few points close to boiling inception fell somewhat above McAdams curve, probably owing to thermocapillary jetting from potential nucleation sites. This process is a Marangoni effect which has been discussed by a variety of investigators (see e.g. Trefethen [20, 21]). Such jetting was evident in our experiments and is discussed at greater length in [18]. For larger heaters, on which R' is small by virtue of low gravity, the conventional natural convection correlations for cylinders should apply perfectly well.

THE INCEPTION OF BOILING

Double equilibrium of unstable nuclei

In 1961, Hsu [22] pointed out that when a nucleus bubble protrudes into liquid with a non-uniform temperature profile at a wall, there are *two* equilibrium positions that it might assume. Brown [23] subsequently described this process for a steady temperature profile, in the following way:

The temperature profile at the wall is given in terms of the heat flux and the distance, y, from the wall, as

$$T = T_w - qy/k. \tag{3}$$

The rate of change of temperature with pressure inside the bubble is given by the Clausius–Clapeyron equation as:

$$\frac{dT}{dp} \simeq \frac{T_{sat} v_{fg}}{h_{fg}}. \tag{4}$$

If we take the right-hand-side of equation (4) as nearly constant over the small temperature ranges of interest, then integrate it between T_{sat} and T of interest, and finally introduce the Laplace equation ($p - p_{sat} = 2\sigma/r$), we get the relation between the temperature in a bubble and its radius, r, as

$$T = T_{sat}\left[1 + \frac{v_{fg}}{h_{fg}}\frac{2\sigma}{r}\right]. \tag{5}$$

Now, with reference to Fig. 16, let us consider a hemispherical nucleus protruding into a liquid whose temperature is given by equation (3). At a point $r = y$, for which the temperatures given by equations (3) and (5) are equal, the cap of the bubble will be in equilibrium. However, the liquid around the equatorial region will be hotter than the gas inside, and evaporation will occur. This will cause the bubble to

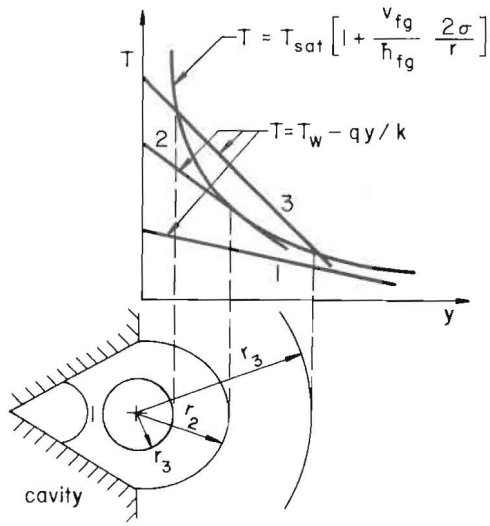

FIG. 16. Equilibrium nucleus radii in a temperature gradient near a wall.

grow a little larger, forcing the cap into cooler liquid until a balance is struck between condensation at the cap and evaporation at the base of the bubble. Thus the equilibrium radius will be just a little in excess of the r for which the T's given by equations (3) and (5) are equal.

Depending upon the parameters of equations (3) and (5), three situations can exist as suggested by Fig. 16. If there is no intersection, the shape of any liquid–vapor interface that might exist in the cavity is determined, not by equations (3) and (5), but by such features of the cavity as the contact angle and the presence of noncondensable gases. If the curves simply fall tangent there is a single equilibrium radius, a little larger than r_2. If the temperature distribution in the liquid near the wall is still steeper, there will then be two possible equilibrium points one of which will be a little larger than r_3. The other equilibrium radius is smaller than the existing site in this case; hence it would have been triggered already in the cavity depicted. If the cavity were smaller, either site could exist.

The double radii are stable with respect to slow changes of q (and of the temperature gradient) until the smaller radius becomes too small for the cavity. The larger radius will trigger if its size is somehow altered quickly enough that inertia will cause it to overshoot its equilibrium. Accordingly the group at M.I.T. named these large nuclei, "metastable bubbles" and they noted experimental examples of their metastable behaviour [23, 24]. We shall have two occasions in the present discussion to point out their influence.

Nucleation hysteresis*

In all cases, nucleation occurred in the present tests at temperatures well in excess of that predicted by equations (3) and (5) for r_2. Furthermore nucleation always began at temperatures a good deal larger than those at which it stopped. Thus a "metastable bubble" undoubtedly gave rise to nucleation, and nucleation terminated when the temperature fell below the triggering temperature for the cavity. The disparity between the two points is called "nucleation hysteresis".

Temperature overshoot hysteresis

The phenomenon of temperature overshoot is well known. In prior studies, we have each noted independently [24, 25] that when nucleation occurs the temperature sometimes drops back before continuing to rise with q. Then, the decreasing heat flux traverse usually drops to the right of the nucleation heat flux and meets the convection regime with much less discontinuity. Several other authors, all the way back to Corty and Faust [26], have noted this hysteresis. In the present case the magnitude of the temperature overshoot diminishes with size as is demonstrated in Fig. 17—a plot of the temperature drop at inception, ΔT_{ov}, against wire size.

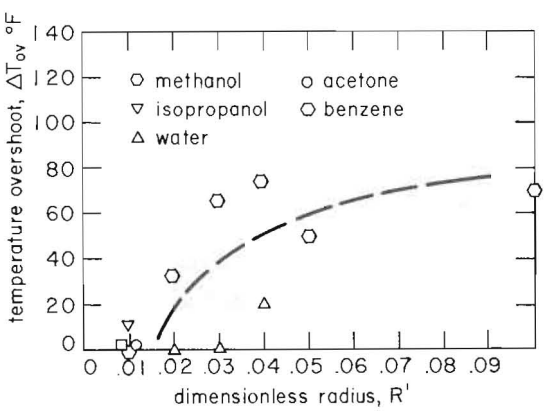

FIG. 17. Influence of heater size on temperature overshoot.

It is commonly argued (see e.g. [26, 27]) that the overshoot occurs because the first nucleation triggers many adjacent sites and a sudden onset of widespread boiling cools the heater. Before the first boiling occurs, the larger

* We use the word "nucleation" to denote the inception of bubble growth whether it leads (as in the case of small R') directly to film boiling or (as in the case of larger R') to nucleate boiling.

nucleation sites which would normally have triggered inception, are initially filled with liquid and they do not function at low temperatures. But as the heat flux is decreased, the sites, having filled with vapor and begun to function, will continue to function down to low temperatures, thus shifting the return traverse to the right and causing a hysteresis. That the temperature overshoot vanishes with decreasing wire size simply reflects the fact that there are fewer and fewer large sites on finely drawn wires.

Thus the nucleation hysteresis should be the same for large wires at low gravity as for these small wires. But the temperature overshoot hysteresis, on the other hand, could not be expected to vanish on large wires at low gravity the way it does here.

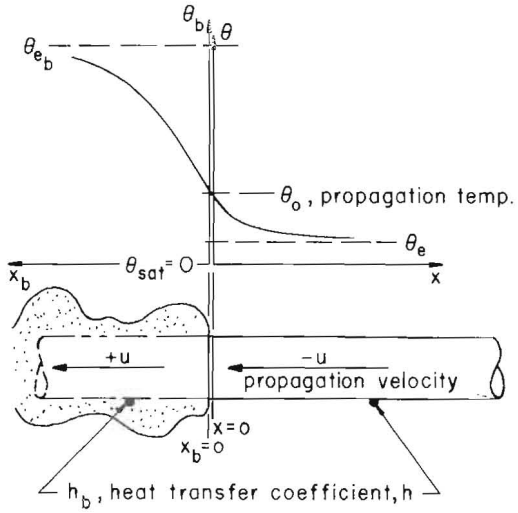

FIG. 18. Steady-state representation of advance of a vapor patch.

MIXED-MODE BOILING

Vapor front propagation

Figure 15 suggests an important aspect in the growth of a vapor patch, namely that it spreads with a constant velocity. This behavior was reproducible in many motion picture runs for wires in methanol and it was evident in the other organic liquids, but not in water. Since this spreading behaviour is a primary feature of the mixed-mode regime we wish to look at it in detail.

Figure 18 shows the advancing vapor patch in a coordinate frame that moves with the speed of propagation, u. Thus the liquid–vapor interface is fixed while the wire moves into it with a speed, u. Defining $\theta \equiv T - T_{sat}$, we can write the equilibrium wire temperatures under the patch and in the liquid as θ_{e_b} and θ_e, respectively.

We propose to determine the propagation or "triggering" temperature θ_0, that is consistent with an observed propagation speed. This will then help to reveal the mechanism of propagation. In particular we wish to know whether the interface propagates at the Leidenfrost temperature or at a nucleation temperature.

The heat conduction equation for the wire is easily obtained from the familiar fin equation as long as the transverse Biot number, hR/k, is small:

$$-\frac{u}{\alpha}\frac{d\theta}{dx} = \frac{d^2\theta}{dx^2} + \frac{2q}{k_w R} - \frac{2h}{k_w R}\theta \qquad (6)$$

where q here designates the local heat flux. It will be less in the unblanketed portion of the wire since the temperature (and electrical resistance) are lower in that portion. Equation (6) will apply to either the blanketed portion of the wire (hereafter designated with the subscript, b) or to the unblanketed portion. The boundary conditions are

$$\theta(\infty) = \theta_e; \qquad \theta_b(\infty) = \theta_{e_b};$$

$$\left.\frac{d\theta}{dx}\right|_{x=0} = \left.\frac{d\theta_b}{dx}\right|_{x_b=0}; \qquad \theta(0) = \theta_b(0) = \theta_0. \qquad (7)$$

The dependence of the propagation velocity upon system variables is given by $u = u(\alpha, q, q_b, k_w, R, h, h_b, \theta_0)$ where θ_e and θ_{e_b} are dependent variables since they equal q/h and q_b/h_b respectively. There are thus 9 variables expressible in 4 dimensions, so the problem reduces to 5

independent dimensionless groups. For these we choose:

$$\Theta_0 \equiv \frac{\theta_0}{q/h} = \frac{\theta_0}{\theta_e}; \qquad Pe \equiv \frac{u}{\alpha\sqrt{(2h/k_wR)}};$$

$$Bi \equiv \frac{hR}{2k_w}; \qquad \frac{h_b}{h}; \qquad \frac{q_b}{q}. \tag{8}$$

The first group is a dimensionless triggering temperature. The second group is a kind of Péclét number involving the familiar fin constant, $\sqrt{(2h/k_wR)}$. It compares the propagation capacity of the vapor front to the conduction capacity of the wire. The Biot number, Bi, is typically on the order of 10^{-3} in the present problem, and should therefore exert no influence other than assuring us that radial conduction can be ignored in the total problem. Thus we anticipate a functional equation of the form:

$$\Theta_0 = \Theta_0(Pe, h_b/h, q_b/q).$$

The analytical problem then reduces to a pair of coupled ordinary differential equations:

$$\Theta'' + Pe\Theta' - \Theta = -1 \tag{9}$$

$$\Theta_b'' - Pe\sqrt{\left(\frac{h}{h_b}\right)}\Theta_b' - \Theta_b = -\frac{h}{h_b}\frac{q}{q_b} = -\theta_{eb}/\theta_e$$

with boundary conditions:

$$\Theta(\infty) = 1; \quad \Theta_b(\infty) = \frac{q_b h}{q h_b};$$

$$\Theta'(0) = -\sqrt{\left(\frac{h_b}{h}\right)}\Theta_b'(0);$$

$$\Theta(0) = \Theta_b(0) = \Theta_0 \tag{10}$$

where the dimensionless dependent variable is $\xi \equiv x\sqrt{(2h/k_wR)}$ or $\xi_b \equiv x_b\sqrt{(2h_b/k_wR)}$. The solution is straight forward and the result is

$$\Theta_0 = \frac{1 - \frac{h}{h_b}\frac{q_b}{q}\left[\frac{1 - \sqrt{(1 + 4h_b/hPe^2)}}{1 + \sqrt{(1 + 4/Pe^2)}}\right]}{1 - \left[\frac{1 - \sqrt{(1 + 4h_b/hPe^2)}}{1 + \sqrt{(1 + 4/Pe^2)}}\right]}. \tag{11}$$

Equation (11) will (by way of an example) now be compared with methanol data for a 1-mil platinum wire (Figs. 5 and 15). To make the comparison we take the blanketed and unblanketed conditions to correspond approximately with the points at either end of the mixed-mode regime in Fig. 5. Here, $h = 1475$ and $h_b = 654$ Btu/ft^{2}h°F, so $h_b/h = 1/2{\cdot}26$. The temperatures at the end points are such that $q_b/q = 1{\cdot}95$.

Figure 19 displays equation (11) for this q_b/q and for three values of h_b/h: 0, $\frac{1}{8}$, and the

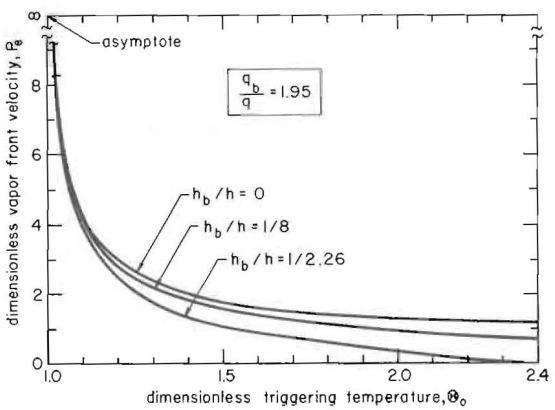

FIG. 19. Influence of triggering temperature on vapor front velocity.

value of 1/2·26 given above. It is clear from the curve that the relation between the dimensionless propagation velocity, Pe, and the triggering temperature, Θ_0, is not too sensitive to h_b/h. In this case the average value of u was found to be about 0·86 ft/s (cf. Fig. 15 where $u =$ 0·83 ft/s) which gives $Pe = 2{\cdot}48$. The corresponding value of Θ_0 is 1·19, so the vapor front propagates by virtue of a triggering temperature only 19 per cent higher than that which gives rise to the first nucleation.

The triggering temperature for methanol is thus comparatively low—a typical nucleation temperature—and definitely not the Leidenfrost temperature. Figure 15 bears this out in

that the front appears to be moving by triggering a succession of new bubbles immediately adjacent to it. The patch spreads until so much of the wire is insulated and heated-up that the resistance rises, throttling the current. This reduces the heat flux and the patch must again retreat. The result is the rapid, and apparently random, growth and collapse of patches on the wire.

Non-propagation of the vapor front

One of the liquids used in the present study—distilled water—did not show the propagation of the vapor patch. The patch (or patches) formed in water and spread in direct proportion to q. The flickering behavior was not present as it was in the various organic liquids.

To see why this should be, we might first recall (Figs. 3–14) that the nucleation hysteresis was far less pronounced in water than in the organic liquids. But nucleation hysteresis should depend on the presence of "metastable bubbles". Let us therefore equate T as given by equations (3) and (5) and set $y = r$. The result can be solved for r, whence:

$$\frac{hr}{k} = \tfrac{1}{2} \pm \sqrt{(\tfrac{1}{4} - \Lambda)} \qquad (12)$$

where

$$\Lambda \equiv 2\sigma h v_{fg} T_{sat}/k h_{fg} \Delta T . \qquad (13)$$

The ratio of the two possible radii given by equation (12) will be real if nucleation occurs. Thus:

$$\frac{r_{big}}{r_{little}} = \frac{1 + \sqrt{(1 - 4\Lambda)}}{1 - \sqrt{(1 - 4\Lambda)}}; \quad \Lambda \leqslant \tfrac{1}{4}. \qquad (14)$$

Equation (14) is plotted in Fig. 20. Values of Λ based on the inception point for the smallest wire in each of the five liquids have been calculated and plotted on this curve. It turns out that the ratio r_{big}/r_{little} ranges between about 60 and 130 for the organic liquids but it is only about 4 for water. Thus there are many large "metastable bubbles" in the organic liquids. These tend to be triggered by the disturbances associated with the advancing vapor front, so the patch keeps over-running itself and then collapsing. Since any metastable bubbles in water differ relatively little from ordinary nuclei, the front can trigger only the nuclei very near the vapor-front and the advance is stable.

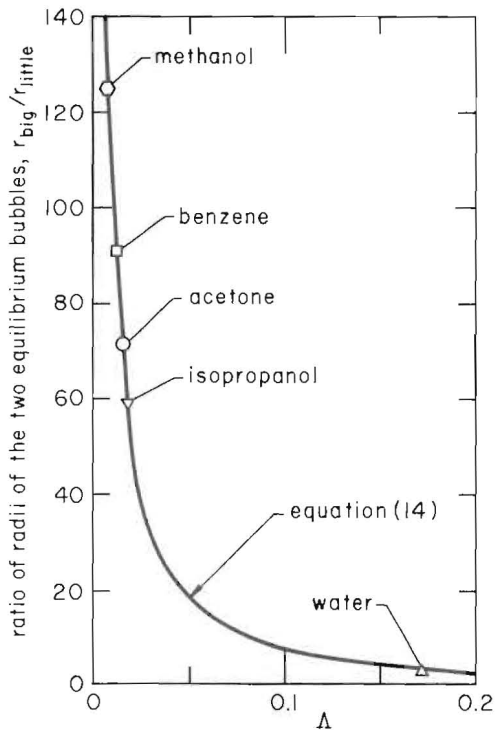

FIG. 20. Radius ratio of equilibrium bubbles at inception for various liquids on small wires.

Using Fig. 7 we find $h_b/h = \frac{1}{8}$ for water on a 2-mil wire. Entering equation (11) with this value and a zero propagation speed (i.e. $Pe = 0$) we find $\Theta_0 \simeq 6{\cdot}6$ or (since $\theta_e \simeq 70\,°\text{F}$) $\theta_0 \simeq 462\,°\text{F}$. The front can thus be at any temperature up to $\theta = 462\,°\text{F}$ but it still is not triggering nuclei. Thus, without large metastable bubbles on the wire, only those nuclei immediately adjacent to the vapor-front will be triggered. Furthermore θ_0 is too low to trigger a Leidenfrost front. This is why the patch doesn't move in this case.

Large cylinders at low gravity would behave like those described here with two possible changes: (1) The Biot number might become large enough to make the heat conduction problem two-dimensional. This would require a considerably more complicated set of predictive relations than we have offered, possibly without great change in the results. (2) With more nucleation sites on the cylinder, θ_0 would probably tend to be lower than it is on small wires.

FILM BOILING

Bromley [28] provided the first analytical prediction of heat transfer from cylinders in 1950. He found that:

$$Nu/(Ra^*)^{\frac{1}{4}} = 0{\cdot}62 \tag{15}$$

where:

$$Ra^* \equiv \rho_g(\rho_f - \rho_g)\, h^*_{fg}\, g(2R)^3/\mu\, k_g\, \Delta T. \tag{16}$$

In 1962, Breen and Westwater [29] provided a semi-empirical modification of Bromley's equation. For $2R' < 0{\cdot}8$ they recommended:

$$Nu/(Ra^*)^{\frac{1}{4}} = 0{\cdot}372(2R')^{\frac{1}{4}} + 0{\cdot}274/(2R')^{\frac{3}{4}}. \tag{17}$$

Finally, in 1967 Baumeister and Hamill [30] derived the following relation

$$Nu/(Ra^*)^{\frac{1}{4}} = 0{\cdot}373\left[(2R') + 3{\cdot}68 + \frac{1{\cdot}088}{(2R')^2}\right]^{\frac{1}{4}}. \tag{18}$$

The present film boiling data have been plotted on $Nu/(Ra^*)^{\frac{1}{4}}$ vs. $(2R')$ coordinates in Fig. 21, and the preceding three expressions have been included for comparison. Bromley's prediction is, of course, low for small R' and the other two expressions were developed with the objective of improving it. Equations (17) and (18) are a little high and a little low respectively, but either is in reasonable agreement with the available data. Since Baumeister and Hamill's expression is based upon an analytical rationalization that applies to wires of any size, the correlation in Fig. 21 should be valid for either large wires at low gravity or small wires under higher gravity.

It is, of course, possible to fit an empirical curve to the data in Fig. 21 and obtain higher

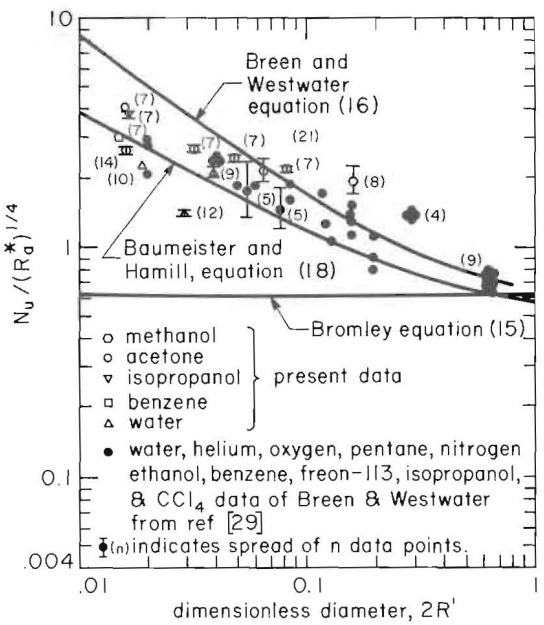

FIG. 21. Correlation of heat transfer data for film boiling on small wires.

accuracy than either equation (17) or (18) will give. For example

$$Nu/(Ra^*)^{\frac{1}{4}} \simeq 0{\cdot}7/(2R')^{\frac{1}{4}} \tag{19}$$

will fit the data nicely.

CONCLUSIONS

(1) The local maxima and minima in the boiling curve which are dictated by hydrodynamic instabilities vanish for all $R' \leqslant 0{\cdot}01$. The region $0{\cdot}01 < R' < 0{\cdot}15$ is a transition regime in which the hydrodynamic mechanisms re-establish themselves.

(2) Nucleate boiling also vanishes when R' becomes small.

(3) Natural convection and film boiling on

small wires (or on larger cylinders at low gravity) are predictable by conventional methods.

(4) The nature of a monotonic boiling curve between first nucleation and full film boiling has been traced in detail and many of its features have been done for the constant electrical current case on small wires. The region is one in which film boiling and natural convection coexist on the wire. If the parameter A is on the order of a few hundredths or less, patches of film boiling flicker on and off over the wire. If A is larger than one or two tenths, the patches are steady and grow only with increasing heat flux. The analytical descriptions of the mixed-mode regime can generally be applied to large cylinders at low gravity as well.

(5) Values of q_{max} hitherto reported by many investigators (e.g. [12–14]) for q_{max} at $R' < 0{\cdot}03$ have probably been either q at the inception of film boiling, or values of q for which the temperature first began to increase rapidly, or possibly values of q for which the heater first glowed red. In any case, such data are not meaningful since there is no longer a real local maximum to measure.

REFERENCES

1. S. NUKIYAMA, The maximum and minimum values of the heat, Q, transmitted from metal to boiling water under atmospheric pressure, *Trans. JSME* **37**, 367 (1934). (Reprinted in *Int. J. Heat Mass Transfer* **9**, 1419–1433 (1966)).
2. T. B. DREW and A. C. MUELLER, Boiling, *Trans. Am. Inst. Chem. Engrs* **33**, 449 (1937).
3. S. S. KUTATELADZE, On the transition to film boiling under natural convection, *Kotloturbostroenie* No. 3, 10 (1948).
4. N. ZUBER, M. TRIBUS and J. W. WESTWATER, The hydrodynamic crisis in the pool boiling of saturated and subcooled liquids, *International Developments in Heat Transfer*, pp. 230–235. ASME, New York (1963).
5. K. H. SUN and J. H. LIENHARD, The peak pool boiling heat flux on horizontal cylinders, *Int. J. Heat Mass Transfer* **13**, 1425–1439 (1970).
6. J. S. DED and J. H. LIENHARD, The peak pool boiling heat flux from a sphere to appear in *A.I.Ch.E.Jl.* (1972).
7. J. H. LIENHARD and P. T. Y. WONG, The dominant unstable wavelength and minimum heat flux during film boiling on a horizontal cylinder, *J. Heat Transfer* **86C**, 220–226 (1964).
8. J. H. LIENHARD and K. H. SUN, Effects of gravity and size upon film boiling from horizontal cylinders, *J. Heat Transfer* **92**, 292–298 (1970).
9. G. I. BOBROVICH, I. I. GOGONIN and S. S. KUTATELADZE, Influence of size of heater surface on the peak pool boiling heat flux, *J. Appl. Mech. Tech. Phys.* No. 4, 137–138 (1964).
10. J. H. LIENHARD and K. WATANABE, On correlating the peak and minimum boiling heat fluxes with pressure and heater configuration, *J. Heat Transfer* **88C**, 94–100 (1966).
11. J. H. LIENHARD, Interacting effects of gravity and size upon the peak and minimum boiling heat fluxes, NASA CR-1551 (May 1970).
12. S. S. KUTATELADZE, N. V. VALUKUNA and I. I. GOGONIN, Influence of heater size on the peak heat flux in saturated liquids, *Inzh. Phyz. Zh.* **12**, 569–575 (1967).
13. R. SIEGEL and J. R. HOWELL, Critical heat flux for saturated pool boiling from horizontal and vertical wires in reduced gravity, NASA Tech. Note TND-3123 (Dec. 1965).
14. C. C. PITTS and G. LEPPERT, The critical heat flux for electrically heated wires in saturated pool boiling, *Int. J. Heat Mass Transfer* **9**, 365–377 (1966).
15. R. SIEGEL and C. USISKIN, Photographic study of boiling in the absence of gravity, *J. Heat Transfer* **81C**, 230–236 (1959).
16. R. SIEGEL and E. G. KESHOCK, Effects of reduced gravity on nucleate boiling bubble dynamics in saturated water, *A.I.Ch.E. Jl* **10**, 509–516 (1964).
17. S. J. D. VAN STRALEN and W. M. SLUYTER, Investigation on the critical heat flux of pure liquids and mixtures under various conditions, *Int. J. Heat Mass Transfer* **12**, 1353–1384 (1969).
18. N. BAKHRU, Heat transfer and boiling from cylinders of small size or under reduced gravity, University of Kentucky College of Engineering, Technical Report UKY 38-71-ME11 (July 1971).
19. W. H. MCADAMS, *Heat Transmission*, 3rd Edition. McGraw-Hill, New York (1954).
20. L. TREFETHEN, *Surface Tension in Fluid Mechanics*, film distributed by Educational Services Inc., Watertown, Mass.
21. L. TREFETHEN, On the jet propulsion of bubbles in a heated liquid, Tufts University, Mechanical Engineering, Report No. 61-S-1 (August 1961).
22. Y. Y. HSU, On the range of active nucleation cavities on a heating surface, *J. Heat Transfer* **84C**, 207–216 (1962).
23. W. T. BROWN, Jr., A study of flow surface boiling, Ph.D. Thesis, Mech. Eng. Dept., Massachusetts Institute of Technology (1967).
24. A. E. BERGLES, N. BAKHRU and J. W. SHIRES, Jr., Cooling of high power density computer components, Tech. Rept. No. 70712-60 Heat Transfer Lab., Mech. Engr. Dept., Massachusetts Institute of Technology (Nov. 1968).
25. H. A. JOHNSON, V. E. SCHROCK, F. B. SELPH, J. H. LIENHARD and Z. R. ROSZTÓCZY, Temperature variation, heat transfer, and void volume development in the transient atmospheric boiling of water, AEC Rept.: SAN-1001 (1961).

26. C. CORTY and A. S. FOUST, Surface variables in nucleate boiling, *Chem. Engng Prog. Symp. Ser.* **51** (17), 1–12 (1955).
27. W. M. ROHSENOW, Heat transfer with boiling, *Modern Developments in Heat Transfer*, edited by W. M. ROHSENOW. The M.I.T. Press (1964).
28. L. A. BROMLEY, Heat transfer in stable film boiling, *Chem. Engng Prog.* **46** (5), 221–227 (1950).
29. B. P. BREEN and J. W. WESTWATER, Effect of diameter on horizontal tubes on film boiling heat transfer, *Chem. Engng Prog.* **58** (7), 67–72 (1962).
30. K. J. BAUMEISTER and T. D. HAMILL, Film boiling from a thin wire as an optimal boundary-value process, ASME Paper No. 67-HT-62 (1967).

EBULLITION A PARTIR DE PETITS CYLINDRES

Résumé—On analyse en fonction de la température le transfert thermique sur des petits fils horizontaux immergés dans l'eau et dans quatre liquides organiques. Quand le rayon du fil est suffisamment petit, les transitions hydrodynamiques dans la courbe d'ébullition disparaissent et la courbe devient monotone. Trois modes d'évacuation de chaleur sont identifiés à partir de la courbe monotone et sont analytiquement décrits: un mode de convection naturelle, un mode mixte d'ebullition en film et de convection naturelle et un mode pur d'ébullition en film. L'ébullition nucléée ne se produit pas sur les petits fils.

Le but de cette étude est la prévision du comportement de grands chauffoirs pour une faible gravitation. L'application des résultats présents à de telles circonstances est discutée. On propose que les flux thermiques maximum et minimum s'évanouissent aussi à faible gravitation comme pour des fils minces.

SIEDEN AN DÜNNEN DRÄHTEN

Zusammenfassung—An dünnen horizontalen Drähten in Wasser und vier organischen Flüssigkeiten wird der Wärmeübergang als Funktion der Temperatur untersucht.

Wenn der Drahtdurchmesser genügend klein ist, verschwinden die hydrodynamischen Übergänge in der Siedekurve und die Kurve wird monoton. Drei Arten des Wärmetransportes wurden für die monotone Kurve gefunden und analytisch beschrieben: eine Art der freien Konvektion, eine gemischte Art von Filmsieden und freier Konvektion und eine Art reinen Filmsiedens. Blasensieden tritt an dünnen Drähten nicht auf.

Die Arbeit wurde angeregt durch das Interesse am Verhalten grosser Heizflächen bei geringer Schwerkraft. Die Anwendung der vorliegenden Ergebnisse unter solchen Bedingungen wird daher diskutiert. Es wird vorausgesetzt, dass die maximalen und minimalen Wärmestromdichten sowohl bei geringer Schwerkraft, als auch an dünnen Drähten verschwinden.

КИПЕНИЕ НА ПОВЕРХНОСТИ НЕБОЛЬШИХ ЦИЛИНДРОВ

Аннотация—Наблюдался теплоотвод от небольших горизонтальных проволочек в воде и четырех органических жидкостях в зависимости от температуры. При довольно малых радиусах проволочки исчезают гидродинамические переходы, и кривая становится монотонной. Аналитически установлены и описаны три способа отвода тепла для случая монотонной кривой: естественная конвекция, смешанное пленочное кипение с естественной конвекцией и чисто пленочное кипение. Пузырьковое кипение на тонких проволочках не происходит. Исследование вызвано интересом, проявляемым к расчету больших нагревателей при малой гравитации. Поэтому обсуждается применение настоящих результатов к таким случаям. Предполагается, что пиковые и минимальные тепловые потоки исчезают при малой гравитации, так же как и на тонких проволочках.